Synthesis of 7-^{15}N-Oroidin and Evaluation of Utility for Biosynthetic Studies of Pyrrole−Imidazole Alkaloids by Microscale ^{1}H−^{15}N HSQC and FTMS†

Yong-Gang Wang,‡ Brandon I. Morinaka,§ Jeremy Chris P. Reyes,‡ Jeremy J. Wolff,⊥ Daniel Romo,*,‡ and Tadeusz F. Molinski*,§,∥

Department of Chemistry, Texas A&M University, P.O. Box 30012, College Station, Texas 77842-3012, Bruker Daltonics, 40 Manning Road, Billerica, Massachusetts 01821, and Department of Chemistry and Biochemistry, and Skaggs School of Pharmacy and Pharmaceutical Sciences, University of California, San Diego, 9500 Gilman Drive, La Jolla, California 92093-0358

Received October 8, 2009

Numerous marine-derived pyrrole−imidazole alkaloids (PIAs), ostensibly derived from the simple precursor oroidin, **1a**, have been reported and have garnered intense synthetic interest due to their complex structures and in some cases biological activity; however very little is known regarding their biosynthesis. We describe a concise synthesis of 7-^{15}N-oroidin (**1d**) from urocanic acid and a direct method for measurement of ^{15}N incorporation by pulse labeling and analysis by 1D ^{1}H−^{15}N HSQC NMR and FTMS. Using a mock pulse labeling experiment, we estimate the limit of detection (LOD) for incorporation of newly biosynthesized PIA by 1D ^{1}H−^{15}N HSQC to be 0.96 μg equivalent of ^{15}N-oroidin (2.4 nmole) in a background of 1500 μg of unlabeled oroidin (about 1 part per 1600). 7-^{15}N-Oroidin will find utility in biosynthetic feeding experiments with live sponges to provide direct information to clarify the pathways leading to more complex pyrrole−imidazole alkaloids.

The polycyclic pyrrole−imidazole alkaloid (PIA) family has received much attention recently from the synthetic organic community[1] because of their challenging molecular structure, dense functionality, and potential biological activity. All are believed to derive from a simple common sponge metabolite, most likely oroidin (**1a**) or its analogues hymenidin (**1b**) and clathrodin (**1c**), the structures of which differ only in bromine content.[2] Representative of the members of this family are the dimeric PIAs sceptrin (**2**),[3] ageliferin (**3**),[4] massadine (**4**),[5] palau'amine (**5**),[6] and axinellamines A and B (**6a**,**b**)[7] and higher-order tetrameric PIAs.[8] In addition, compact monomeric polycyclic PIAs, such as agelastatins A,[9] B,[10] C, and D[11] (**7a**−**d**) and dibromophakellin[12] appear to be derived from oxidative intramolecular cyclizations of oroidin (**1a**) or hymenidin (**1b**). PIAs are of contemporary interest due to their potent biological activity and intriguing biosyntheses. For example, (−)-agelastatin A (**7a**), an antitumor PIA,[10] is 1.5−16 times more active than cisplatin against a range of tumor cell lines and potently inhibits osteopontin, an adhesion glycoprotein transcriptionally regulated by the Wnt β-catenin pathway and implicated in tumor progression, dissemination, and metastases.[13]

The widely accepted hypothesis for biosynthesis of dimeric and tetrameric PIAs involves dimerization of oroidin (**1a**) followed by consecutive oxidative transformations leading to more densely functionalized polycyclic alkaloids.[8] In 1982, Büchi reported a "biomimetic" synthesis of the simple PIA racemic dibromophakellin by oxidative cyclization of 9,10-dihydrooroidin.[14] The structure of sceptrin (**2**) is highly suggestive of a formal [2+2] cycloaddition of two molecules of hymenidin (**1b**) to **2**; however, despite many attempts, Faulkner, Clardy, and co-workers were unable to achieve photodimerization of **1b** to **2**,[3] suggesting that an alternative nonconcerted mechanism may be responsible for the biosynthesis. Recent speculation on the order of biosynthesis of **2** and **3** revolves around ionic mechanisms of ring expansion, supported by the demonstrated conversion of **2** to **3** under thermal conditions,[1f,15,16] or a ring-contraction pathway from an ageliferin-type dimer generated by a Diels−Alder-type cycloaddition of two molecules of hymenidin (**1b**).[2] For example, one speculative hypothesis invokes a cycloaddition in the biosynthesis of palau'amine[6b] and axinellamine, followed by a stepwise electrophilic chlorination and ring contraction. Remarkably, none of the above hypotheses have been tested experimentally in live sponges.

We describe here a synthesis of ^{15}N-labeled oroidin (**1d**) and optimization of conditions for detection of ^{15}N-incorporation by microscale FTMS and ^{1}H−^{15}N HSQC using a "mock" pulse-labeling experiment with **1d** and natural oroidin (**1a**). We estimate the limits of detection of these methods and determine their suitability for use in field incorporation for biosynthetic studies of complex PIAs with living sponges. This information can be used to answer questions of the biosynthesis of PIAs by sponges in the genera *Agelas*, *Stylissa*, and *Ptilocaulis*.

Results and Discussion

Several syntheses of oroidin have been described in the literature, and the synthetic approaches utilized can be classified into two categories.[17] The first involves synthesis of the required 2-aminoimidazole ring by condensation of a guanidine derivative[18] or cyanamide[19] with an α-haloketone. An alternative strategy involves amination of an imidazole ring via azido or diazonium transfer reagents.[20] We elected the latter strategy for brevity and the utility of the commercially available starting material urocanic acid, as demonstrated by Lovely.[1o,21] This strategy enabled a late-stage introduction of the ^{15}N-label, which is ideal for cost considerations (Scheme 1). Disconnection of the amide bond leads to the known 4,5-dibromo-2-trichloroacetylpyrrole **8**,[21] readily synthesized from commercially available 2-trichloroacetylpyrrole, and the ^{15}N-labeled allylic amine **9**, which could be obtained by a lithiation/azidation sequence at the 2-position of the *N*-protected urocanic acid ester **10**. The ^{15}N label would be introduced toward the end of the overall sequence by Gabriel synthesis employing the potassium salt of commercially available ^{15}N-phthalimide and an activated derivative of the alcohol, which, in turn, could be obtained by reduction of the carbomethoxy group of ester **10**.

Fisher esterification of urocanic acid with methanol (Scheme 2) and subsequent protection gave the known *N*-trityl imidazole

† Dedicated to the late Dr. John W. Daly of NIDDK, NIH, Bethesda, Maryland, and to the late Dr. Richard E. Moore of the University of Hawaii at Manoa for their pioneering work on bioactive natural products.

* To whom correspondence should be addressed. Tel: +1 (858) 534-7115. Fax: +1 (858) 822-0386. E-mail: tmolinski@ucsd.edu. Tel: +1 (979) 845-9571. Fax: +1 (979) 862-4880. E-mail: romo@tamu.edu.

‡ Texas A&M University.

§ Department of Chemistry and Biochemistry, UC San Diego.

⊥ Bruker Daltonics.

∥ Skaggs School of Pharmacy and Pharmaceutical Sciences, UC San Diego.

10.1021/np900638e
Published on Web 01/22/2010

Scheme 1. Retrosynthetic Analysis of 7-^{15}N-Oroidin (**1d**) from Urocanic Acid

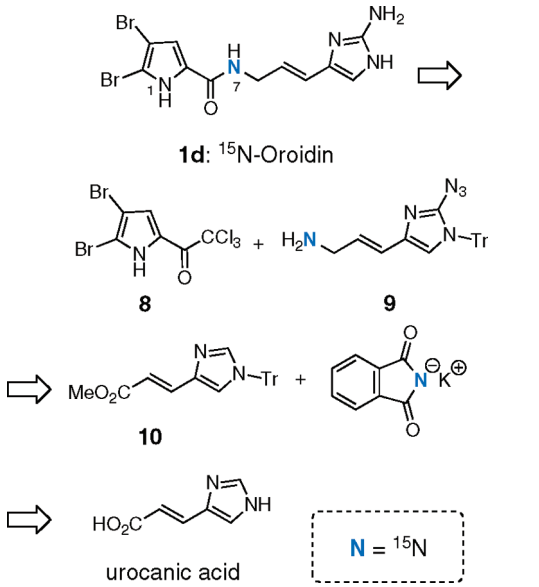

Scheme 2. Synthesis of ^{15}N-Labeled Oroidin[a]

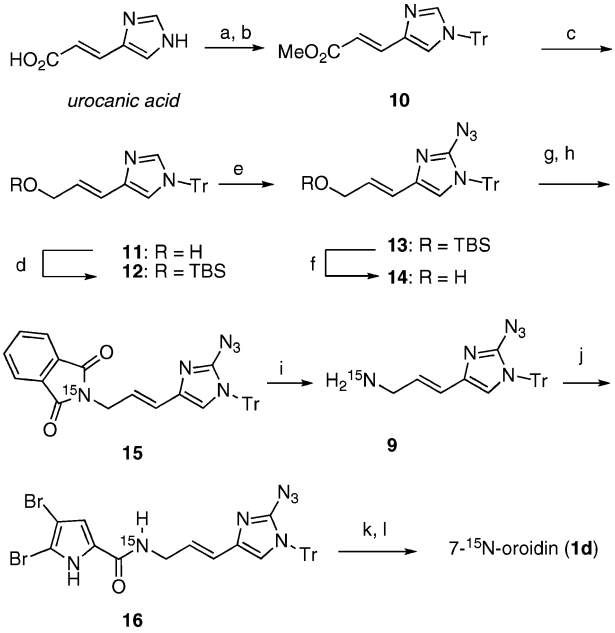

[a] Reagents and conditions: (a) AcCl, MeOH, reflux, quant.; (b) TrCl, Et_3N, DMF; (c) DIBAL-H, THF; (d) TBSCl, imidazole, 74% for 3 steps; (e) *n*-BuLi, TsN_3, THF, 94%; (f) TBAF, THF, 82%; (g) MsCl, Et_3N, THF; (h) potassium phthalimide-^{15}N, DMF, 42% for 2 steps; (i) NH_2NH_2, EtOH, 50 °C; (j) 4,5-dibromo-2-trichloroacetylpyrrole, Na_2CO_3, DMF, 76% for 2 steps; (k) AcCl, MeOH/EtOAc, 99%; (l) H_2/Pd-Lindlar, MeOH/THF, 84%.

derivative **10**.[22] Reduction of ester **10** (DIBAL-H) afforded the corresponding alcohol **11** in excellent yield. Initial attempts to execute a direct azidation of alcohol **11** at the 2-imidazole position with the unprotected alcohol using known procedures (*n*-BuLi/TsN_3)[20c−e] gave none of the desired azido product. Instead, the product obtained was tentatively assigned the structure of a triazene-imidazole derivative based on ^{1}H NMR and mass spectrometric analysis.[23] When the TBS-protected imidazole **12** was subjected to the previously employed conditions for azido transfer, azide **13** was obtained in excellent yield. Deprotection of silyl ether **13** with TBAF afforded alcohol **14**, which was then subjected to mesylation (MsCl, Et_3N). Without purification, the mesylate was treated with the potassium salt of ^{15}N-phthalimide (>98% atom ^{15}N) to provide

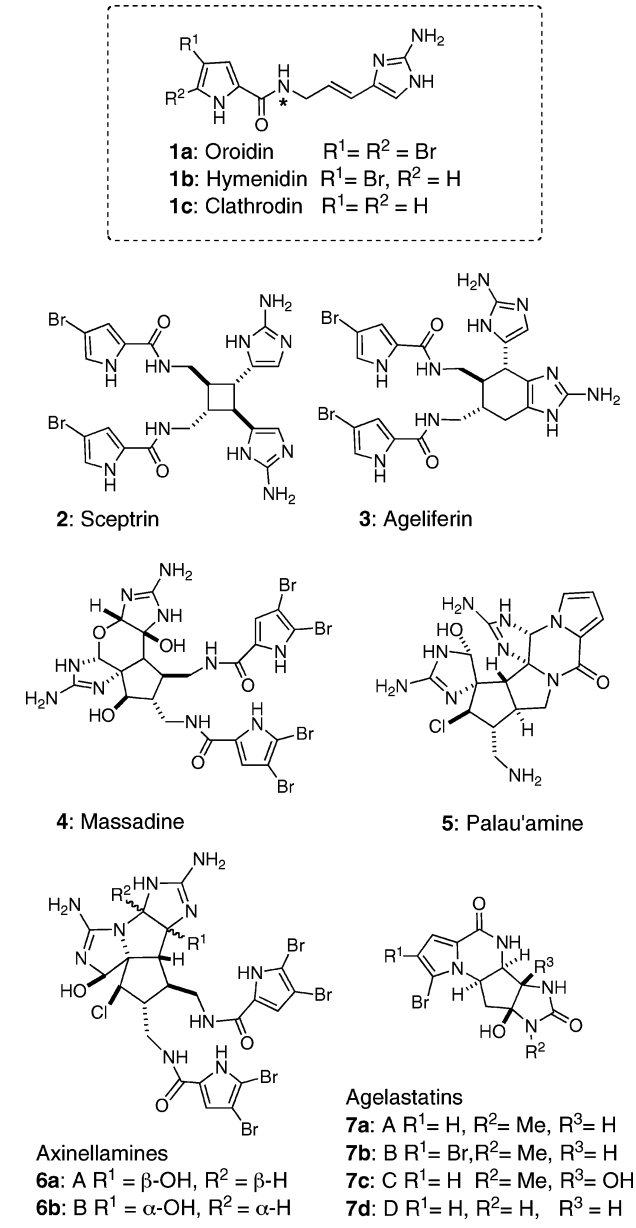

Figure 1. Oroidin (**1a**) and other representatives of the pyrrole−imidazole alkaloid (PIA) family from marine sponges.

the ^{15}N-labeled pthalimide **15**. Cleavage of phthalimide **15** with NH_2NH_2 furnished the ^{15}N-allylic amine **9**, which was acylated with 4,5-dibromo-2-trichloroacetylpyrrole (**8**) to provide ^{15}N-pyrrole-carboxamide **16** in good overall yield. Removal of the trityl group from **16** with anhydrous methanolic HCl, generated in situ from acetyl chloride and MeOH, afforded the corresponding 2-azido imidazole,[20c] which was hydrogenated in the presence of Lindlar's catalyst to provide 7-^{15}N-oroidin (**1d**, >98% atom ^{15}N).

The ^{1}H, ^{13}C, and ^{15}N NMR spectra and mass spectra were fully consistent with the structure and location of the ^{15}N label as depicted. The FTMS of natural oroidin (**1a**, Figure 1) shows the expected 1:2:1 pattern for the pseudomolecular ion $[M + H]^+$ associated with the ^{79}Br and ^{81}Br isotopomers (*m/z* 387.93990, Δmmu = −0.41 mmu). The FTMS spectrum of 7-^{15}N-oroidin (**1d**) (Figure 2b) shows the same ion pattern, except the distribution is increased by 1 amu (*m/z* 388.93719, Δmmu = −0.16). Less than 2% of the ^{14}N isotopomer was detected, which is consistent with the reported purity of the ^{15}N-pthalimide (>98% atom ^{15}N) employed in the synthesis.

Two general methods are available for measuring incorporation of the stable isotope ^{15}N into natural products by pulse labeling:

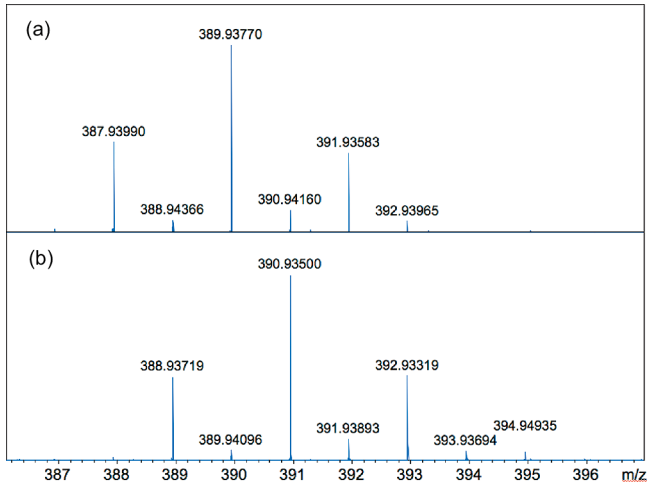

Figure 2. MALDI FTMS (7 T) expansions of the pseudomolecular ion $[M + H]^+$ of oroidin for (a) natural **1a** ($C_{11}H_{12}Br_2{}^{14}N_5O$) and (b) 7-^{15}N-oroidin (**1d**), $C_{11}H_{12}Br_2{}^{14}N_4{}^{15}NO$, >98% atom ^{15}N. Mass accuracy = 1 ppm.

mass spectrometry and NMR. In both techniques, the level of isotopic enrichment from de novo biosynthesis of derived PIAs must exceed the background ^{15}N present of extant PIAs within the sponge *and*, for MS in particular, ^{15}N background contributions from other nitrogen atoms in the molecule. As a stable isotope label, ^{15}N is preferable to ^{13}C because the natural abundance of the heavier to lighter isotope for N (~0.3%) is only about one-fourth of C (~1.1%). ^{15}N incorporation will, therefore, be easier to detect. Ideally for ^{15}N incorporation experiments, mass spectrometry should differentiate the contributions to the M + 1 peak from ^{15}N and ^{13}C,[24] a task best suited to Fourier transform MS (FTMS) with exceptionally high resolution (7 T field, R = 240 000), which should be capable of resolving the nominal M + 1 peak of the pseudomolecular ion into individual isotopomer contributions from species containing one ^{13}C or one ^{15}N. Baseline separation of the isotopomers was readily achieved by MALDI FTMS (Figure 3), allowing quantitation of the ^{15}N isotopomer peak. For oroidin (**1a**), the critical *difference* in the mass of ^{12}C−^{15}N containing ions versus the heavier ^{13}C−^{14}N isotopomer amounts to only 0.00632 amu, a baseline separation not readily achievable by high-resolution mass spectrometers with conventional analyzers (e.g., double sector, TOF).

Quantitation of the ^{15}N isotopomer can be made from integration of ion current intensities of the [M + 1] components, ^{15}N−^{12}C and ^{14}N−^{13}C (Figure 3). Assuming the ^{13}C abundance in *natural* and *synthetic* ^{15}N-labeled oroidin are identical, the ^{13}C peak intensity may be used as the denominator in the ratio h (eq 1), where h_N and h_C are the respective measured peak heights of the ^{15}N−^{12}C and ^{14}N−^{13}C component ions.

$$h = h_N/h_C \quad (1)$$

Consequently, h can be used to reflect small changes in the ^{15}N content.[25] From the ion current peak heights measured in the FTMS spectrum of natural oroidin (**1a**), h was found to be 0.1487 ± 0.0175. A prepared "mock" labeled sample (Mix1), consisting of a 1:0.005 mixture of oroidin (**1a**) and 7-^{15}N-oroidin (**1d**), showed an enhanced h of 0.1881 ± 0.0135, corresponding to a ~4% ^{15}N enrichment. A second sample (Mix2, 1:0.100 **1a**:**1d**) gave h = 1.024 ± 0.0369, corresponding to ~88% ^{15}N enrichment. We estimate that the limit of detection (LOD, ±3σ) for ^{15}N incorporation corresponds to an increase in intensity, Δh ~5.2%. Given that natural abundance of ^{15}N is approximately 0.3% atom, this would amount to observation of as little as 10.4 parts per thousand of ^{15}N incorporation per N atom of oroidin (**1a**) by de novo synthesis. Detection of this small amount will, of course, be made more difficult by the presence of unlabeled oroidin (**1a**) within the sponge.

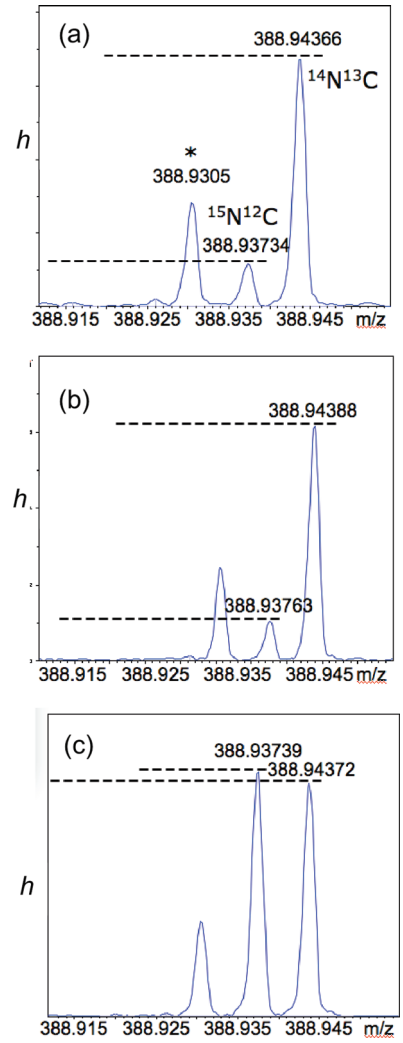

Figure 3. MALDI FTMS (7 T) expansions of m/z and peak height, h, for the M + 1 peak of the pseudomolecular ions of oroidin ($C_{11}H_{11}Br_2N_5O$). Mass accuracy = 1 ppm (R = 240 000). (a) Natural **1a**. (b) **1a** + **1d** (0.04 molar equiv). (c) **1a** + **1d** (0.10 molar equiv). Peak assignments of $[M + H]^+$ in (c): m/z 388.94372, $^{12}C_{10}{}^{13}CH_{12}Br_2N_5O^+$; m/z 388.93739; $^{12}C_{11}H_{12}Br_2N_4{}^{15}NO^+$. The unrelated peak at m/z 388.9305 (indicated with an *) is tentatively assigned to some loss of H from the dominant ^{79}Br/^{81}Br isotopomer, $C_{11}H_{10}{}^{79}Br{}^{81}BrN_5O^+$ ($[M]^+$, Δmmu = −0.5).

The disadvantage of analysis of ^{15}N-content in oroidin and other PIAs by MS is the presence of at least five N atoms, each contributing to the intensity of the ^{15}N−^{12}C component of the M + 1 peak. Consequently, it may be expected that the actual LOD by FTMS will be higher.

Direct detection of ^{15}N incorporation by ^{15}N NMR spectroscopy is impractical due to low natural abundance and severely compromised sensitivity of this I = 1/2 nucleus, which possesses a low-magnitude, negative magnetogyric ratio (γ = −4.31726570 MHz T^{-1}).[26] Conveniently, ^{1}H−^{15}N HSQC circumvents most of these problems by indirect detection of bonded ^{1}H−^{15}N couplets through magnetization transfer from ^{15}N and observation of the more sensitive ^{1}H nucleus. Because four of the five N atoms in oroidin (**1a**) are bonded to H, 2D ^{1}H−^{15}N HSQC can provide bond-specific information about fractional enrichment at an individual N atom in oroidin and, by extension, more complex PIAs by measurement of the ^{1}H−^{15}N couplet intensity. The intensity of cross-peaks in the 2D ^{1}H−^{15}N HSQC spectrum of oroidin will vary for each N−H couplet depending on efficiency of magnetization transfer that largely depends upon the magnitude of the $^1J_{NH}$ scalar coupling

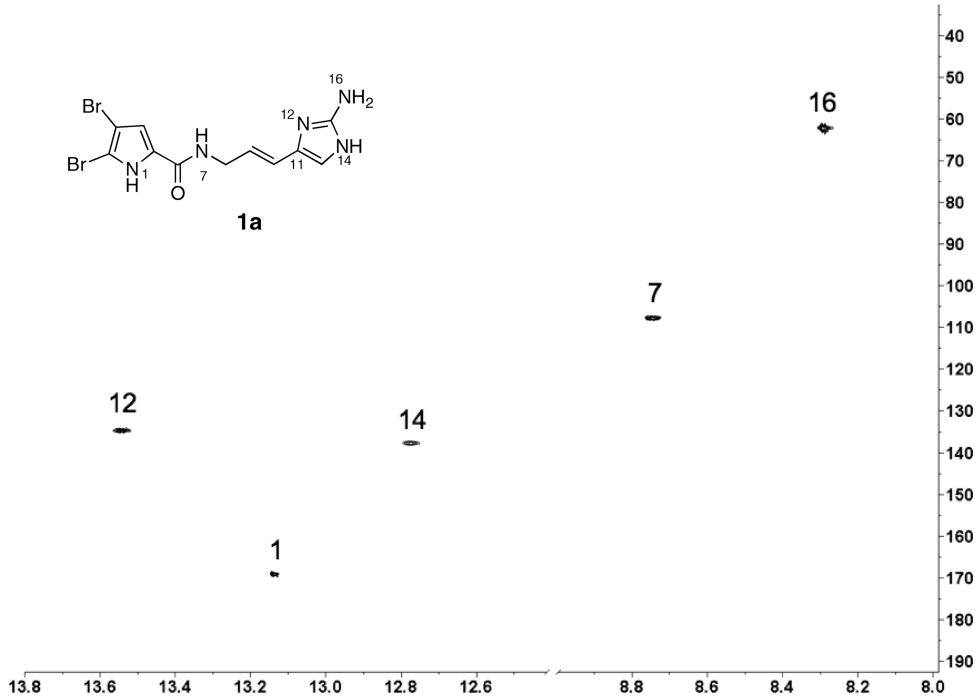

Figure 4. 2D ^{1}H−^{15}N HSQC (600 MHz, 1:1 DMSO-d_6/benzene-d_6) of natural oroidin (**1a**, depicted tautomer is arbitrary). N locants are labeled following the numbering scheme of Assman and Köck (ref 32). ns = 16, T2, T1 = 2K × 256; F2, F1 = 2K × 1K; d1 = 1.5 s.

constant. Nevertheless, the intensity of each cross-peak will scale linearly as a function of ^{15}N abundance.

When put to practice, it is easier and more meaningful to measure ^{15}N enrichment from the volume integration of cross-peaks of 2D HSQC spectra or—best of all—from the 1D version of the HSQC experiment, where evolution of the F1 dimension (^{15}N chemical shift) is eliminated and acquisition time is devoted to improving S/N in the detected dimension F2 (^{1}H chemical shift). We define here ΔI as the *difference* of cross-peak intensity, I, of the ^{15}N-labeled N−H couplet of interest (in this case, the NH(C═O) signal of **1d**) in a sample of oroidin (**1a**), spiked with a known amount of 7-^{15}N-oroidin (**1d**), compared to the intensity, I_0, of oroidin recorded under the same conditions (eq 2). The values of I are normalized to the intensity of the pyrrole N−H couplet of oroidin, I_{py}, in each experiment.

$$\Delta I = (I - I_0)/I_0 \qquad (2)$$

We elected to use the pyrrole N−H couplet of oroidin (**1a**) (δ_H = 13.14, s; δ_N 169.1) as the control because of its ready assignment from ^{1}H−^{15}N HMBC, lack of tautomerism, and likely origination in a different pathway unaffected by biosynthetic incorporation of ^{15}N into the amino-imidazole fragment (see discussion).

The exquisite mass sensitivity of the triple-tuned {^{13}C,^{15}N}^{1}H 1.7 mm 600 MHz microcryoprobe was used to full advantage in this work for characterization of the ^{15}N content of oroidin samples. This low-volume, high-mass sensitivity cryoprobe allowed measurements of samples of only ∼1.5 mg in 35 μL (acquisition times, ∼4 h). Figure 4 shows the 2D ^{1}H−^{15}N HSQC experiment for oroidin (**1a**) with respective N assignments (also, see the Experimental Section for accurate δ's). A single dominant cross-peak was observed in the 2D ^{1}H−^{15}N HSQC of 7-^{15}N-oroidin (**1d**) (not shown), confirming the location of the ^{15}N label at the amide group N−H (δ_H = 8.75, t, $^{3}J_{HH}$ = 6.0 Hz, H7; δ_N = 107.8, N7), as expected.

Figure 5a−c shows 1D ^{1}H−^{15}N HSQC experiments of oroidin (**1a**) spiked with different amounts of 7-^{15}N-oroidin (**1d**), and the signals of each N−H couplet, normalized to the N1-pyrrole couplet, are reported in Table 1 (note that the integrals are not exactly

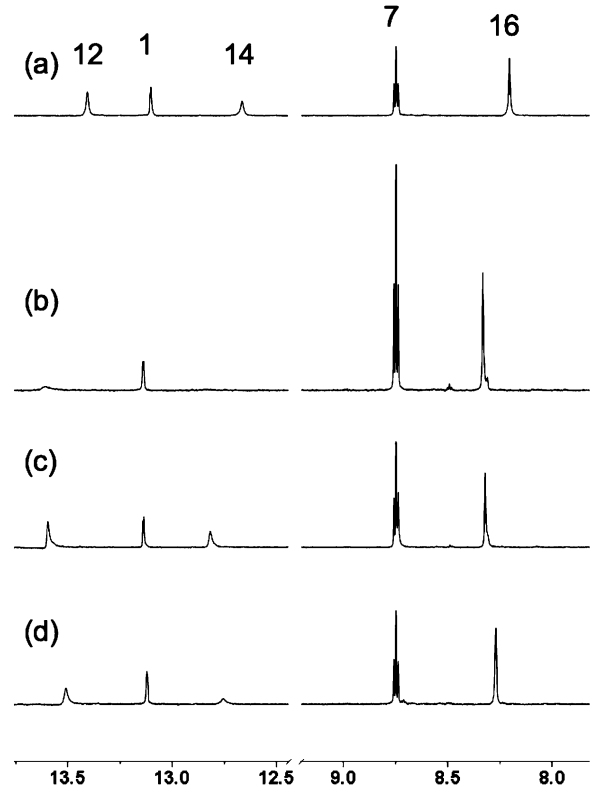

Figure 5. 1D ^{1}H−^{15}N HSQC experiments (^{1}H δ, 1.7 mm microcryoprobe, 600 MHz) of **1a** with N−H assignments. Labels indicate N atom assignments made from a separate ^{1}H−^{15}N HMBC experiment (not shown). (a) 1500 μg of **1a**, no added [^{15}N]-**1d**. (b) 1500 μg **1a** + 10 μg **1d**. (c) 1500 μg **1a** + 5.0 μg **1d**. (d) 1500 μg **1a** + 2.5 μg. Relaxation delay, d1 = 1.50 s, optimized for $^{1}J_{N-H}$ = 90 Hz; ^{1}H π/2 pulse = 12 μS, ^{15}N π/2 pulse = 34 μS; NA = 6K; dummy scans = 16; NI = 1; T2 = F2 = 8K points (no zero fill). See Supporting Information for calculations of limit of detection, mean and SD.

Table 1. Integrals from $^{1}H-^{15}N$ 1D HSQC of Natural Oroidin (**1a**, 1.5 mg/ 30 μL) and **1a** Spiked with **1d**[a]

aliquot μg **1d**	N-12	N-1	N-14	N-7	N-16
0.0	1.26	1.00	1.05	2.17	2.14
2.5	1.03	1.00	0.48	2.57	2.23
5.0	1.65	1.00	1.18	3.83	2.55
10.0	0.63	1.00	0.00	5.74	3.02

[a] Integrals of H−N couplets corresponding to N-12, N-14, and N-16 vary due to tautomerism.

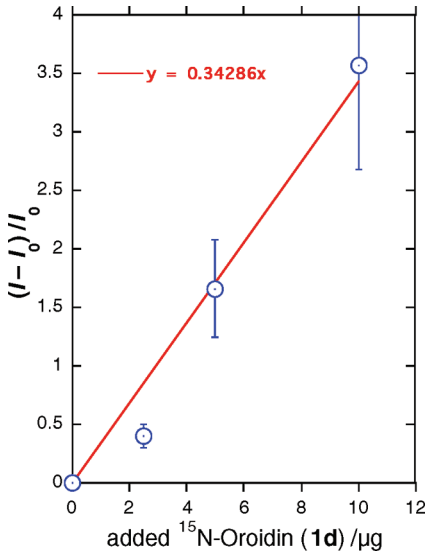

Figure 6. Linear regression of $^{1}H-^{15}N$ HSQC cross-peak integral ratio, $(I - I_0)/I_0$, for the NH(C═O) signal in "mock" pulse-labeling experiments with natural abundance **1a** (1500 μg, I_0) spiked with measured aliquots of **1d** (μg, *x*-scale). Observed values, *I*, for the NH-C═O $^{1}H-^{15}N$ couplet are normalized to the intensity I_{py} of the pyrrole N−H cross-peak. For the NH(C═O) peak in the natural abundance sample (no added **1d**), $I = I_0$ and $I_0/I_{py} = 1.00$. Error bars are ±SD.

proportional to the stoichiometric ratios of attached H's). As predicted, the value of ΔI increases linearly with the amount of added 7-^{15}N-oroidin (**1d**), and the slope of this "standard addition" linear regression (Figure 6) gives the proportionality constant $c = 0.34$ for ΔI per μg of added **1d**. It should be noted that this value will be highly dependent upon the pulse sequence parameters and conditions used for NMR acquisition.

Constant *c* will be useful for estimation of absolute %N incorporations in PIAs labeled during in-field incorporation experiments of secondary metabolism within living sponges. Although it is advisible to measure the relative HSQC intensities of the pyrrole N−H couplet and NH(C═O) couplets of the specific PIA in question, it may be reasonably expected that the magnetic properties of these couplets in more complex PIAs are comparable to those of oroidin (**1a**). We estimate the limit of detection for ^{15}N enrichment by HSQC in **1a** to be approximately 1.5 parts per thousand (based on ±3 SD). This is *more sensitive* than the LOD of ^{15}N-enrichment by FTMS, the reason being that HSQC detects the couplet $^{15}N-^{1}H$ at each N atom and eliminates background "dilution" by other ^{15}N's; however the precision is inferior to FTMS replicate measurements.

Biosynthetic Considerations. Two phases of PIA biosynthesis can be considered: the assembly of oroidin (**1a**) and downstream conversion of the latter to more complex PIAs. Despite much speculation on the biosynthesis of PIAs, only one experimental study in living marine sponges has appeared to date. The precursor for the imidazole side chain is probably an amino acid, and both histidine and ornithine have been proposed.[27] Kerr and co-workers found that cultured cells of *Teichaxinella morchella* (*Stylissa caribica*[28]) produced ^{14}C-labeled stevensine (**17**),[29] the simplest monomeric PIA related to oroidin (**1a**), upon exposure to U-^{14}C-labeled histidine or C5-^{14}C-ornithine, but not U-^{14}C-arginine (Figure 7).[27] Paradoxically, U-^{14}C-histidine was incorporated into **17**, but this would require an additional C_1 unit from an unidentified source to complete the imidazole ring and a nonintuitive substitution of NH_2 at C-2 of the imidazole ring. No simple mechanism for this scenario presents itself. Alternatively, citrulline from the *N*-carbamoylation of ornithine may be the precursor to the side chain of oroidin; however ornithine is also a precursor for the biosynthesis of the pyrrole group. This hypothesis would not be resolved by labeled ornithine incorporation experiments. Ornithine, if it is the precursor to oroidin (**1a**), must undergo decarboxylation, amide coupling with a suitable pyrrole carboxylate group, *N*-carbamoylation to citrulline, oxidative *N*-insertion into the side chain, and aromatization of the heterocyclic product to give the nascent 2-aminoimidazole ring (Figure 7).

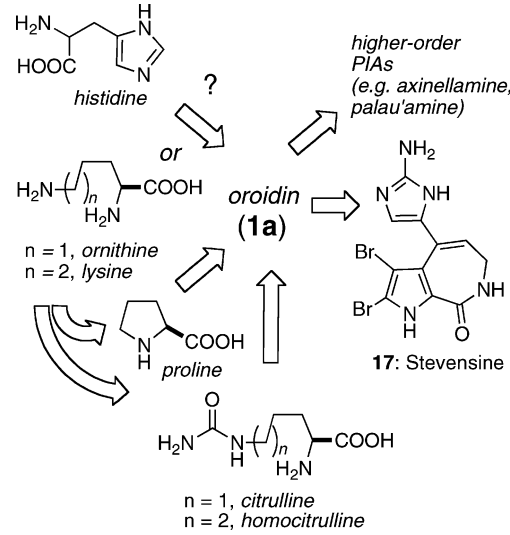

Figure 7. Possible biosynthesis of oroidin (**1a**) and conversion to stevensine (**17**).

These uncertainties in the origin of oroidin (**1a**) are, in theory, addressable by suitable ^{15}N-labeled amino acid incorporation experiments. Unfortunately, low levels of radioactivity and specific incorporation levels were observed with amino acids in the Kerr experiment ([U-^{14}C]-His, 1460 dpm (0.026%) and [U-^{14}C]-ornithine, 1300 dpm (0.024%), respectively[27]), presumably a consequence of the low numbers of cultured cells used (5×10^7) and higher metabolic mobilization and dilution of ^{14}C-labeled amino acids into other committed pathways of primary metabolism. Consequently, detection of ^{15}N incorporation into PIAs using ^{15}N-labeled amino acids may be precluded by the limits of detection. For the above reasons, late-stage precursors (e.g., 7-^{15}N-oroidin (**1d**), sceptrin (**2**), and ageliferin (**3**)) are attractive for mapping the origin of downstream polycyclic PIAs since these molecules should be committed intermediates. Measurement of their rates of incorporation into PIAs in living sponges of the genera *Agelas*, *Stylissa*, and *Ptilocaulis* may also provide critical data on the rates of marine alkaloid secondary metabolism, for which there is no current information.

The use of precursors labeled with the spin $I = 1/2$ stable isotope ^{15}N is particularly attractive, as it provides bond-specific information regarding the flow of intermediates in the biosynthesis of complex PIAs. Judicious design and placement of the label in ^{15}N-labeled oroidin is important. Because the primary NH_2 group of the aminoimidazole group is potentially metabolically labile through deamination reactions, we chose to label the amide bond in ^{15}N-oroidin. Quantitation of ^{15}N incorporation into proteins has been made from integration of cross-peak volumes of 2D HSQC

experiments;[30] however, in the present work with natural products we show that it is far simpler to integrate the corresponding 1D HSQC spectra.

Finally, although the ratio of sceptrin to ageliferin found in one sample of *Agelas conifera* is ~10:1,[31] the ratios of monobrominated and dibrominated analogues of sceptrin and ageliferin vary slightly from approximately 1:1 to 3:4; however, these data do not clearly indicate an ordering for a bromination−dimerization sequence in the biosynthesis of dimeric PIAs. Propagation of 7-^{15}N-oroidin (**1d**) along the biosynthetic pathway to complex PIAs will carry the ^{15}N label through symmetrical and nonsymmetrical intermediates, and detection of residual ^{15}N in strategically chosen N−H bonds in the molecule should reveal timing, ordering, and molecularity of the C−C bond-forming events and the extent of coupling of de novo enzymatic reactions. HPLC analysis of PIA-containing extracts from *A. conifera* (Agelasidae), collected in the Florida Keys by Köck and co-workers,[31] shows the presence of sceptrin (**2**) and ageliferin (**3**); however, some specimens of *Agelas sceptrum* collected by us contained sceptrin (**2**) but were devoid of the expected precursors **1a**−**c**. If **1a**−**c** are precursors to other PIAs, as is highly probable, this implies that the *rates* of conversion of **1a**−**c** to higher-order PIAs are highly dependent upon the sponge species, their biosynthetic capacities, and possibly the habitats they occupy. 7-^{15}N-Oroidin (**1d**) should find great value in systematic studies of the time-dependent biosynthesis of PIA natural products by pulse labeling in live sponges to answer some of these questions.

Conclusion

A concise, gram-scale synthesis of ^{15}N-labeled oroidin from commercially available and inexpensive urocanic acid has been achieved. ^{15}N-Oroidin, or its debromo analogues, may be utilized in biosynthetic feeding experiments to elucidate likely intermediates in the biosynthesis of complex members of the pyrrole−imidazole marine alkaloid family, including palau'amine and axinellamine. FTMS detection of ^{15}N offers unparalleled sensitivity (picomole), and ^{1}H−^{15}N HSQC provides bond-specific information. The utility of ^{1}H−^{15}N HSQC experiments for detection of site-specific ^{15}N incorporation in a mock pulse-labeling experiment has been demonstrated. Several advantages of ^{15}N pulse labeling of biosynthetic pathways are apparent, especially for in-field experiments carried out with living marine invertebrates. The ^{15}N NMR chemical shift was exploited through indirect ^{1}H−^{15}N HSQC to afford enhancement of otherwise weak ^{15}N signals by polarization transfer through N−H couplets. ^{15}N incorporation was further amplified by the enhanced mass sensitivity of the triple-tuned ^{1}H{^{13}C,^{15}N} 600 MHz 1.7 mm microcryoprobe. Biosynthetic studies with alkaloids bearing N−H groups that are not complicated by exchange or tautomerism afford the best cases for application of the technique. In principle, even alkaloids lacking N−H couplets (tertiary N compounds) are amenable to study by detection of long-range ^{1}H−^{15}N couplets from HMBC experiments. The use of ^{15}N stable isotope avoids more complex logistics associated with radioactive tracers (e.g., ^{14}C, ^{3}H) that often preclude laboratory operations aboard seagoing research vessels. The results of field incorporation experiments with 7-^{15}N-oroidin (**1d**) will be reported in due course.

Experimental Section

General Experimental Procedures. IR spectra were recorded on thin films using a Jasco 4100 FTIR by attenuated total reflectance (ATR) on samples mounted on a 3 mm ZnSe plate. ^{1}H and ^{13}C NMR spectra were recorded on a Bruker DRX 600 MHz equipped with 1.7 mm {^{13}C,^{15}N}^{1}H 600 MHz CPTCI microcryoprobe, JEOL 500 MHz spectrometer equipped with a 5 mm {^{13}C }^{1}H probe, or Varian 400 and 500 MHz spectrometers equipped with a 5 mm {^{13}C}^{1}H room-temperature probe and 5 mm {^{1}H}^{13}C cryoprobe, respectively. NMR spectra are referenced to residual solvent signals ($CHCl_3$, ^{1}H, δ 7.26 ppm; $CDCl_3$, ^{13}C, δ 77.16 ppm) or the internal offset for ^{15}N assigned by the instrument manufacturer (Bruker). HRMS measurements of synthetic compounds were made at the Laboratory for Biological Mass Spectrometry (Texas A&M University), Scripps Research Institute (TOF-MS), or University of California, San Diego (EIMS) mass spectrometry facilities. MALDI FTMS were recorded on a 7 T Bruker Apex QFTMS. LCMS was carried out on a ThermoFisher Accela UHPLC coupled to an MSQ single quadrupole mass spectrometer operating in positive ion mode, unless otherwise stated. Semipreparative HPLC was carried out on a Varian SD200 system equipped with a dual-pump and UV-1 UV detector under specified conditions. All solvents for purification were of HPLC grade. See Supporting Information for other procedures.

Synthesis of 7-^{15}N-Oroidin (1d). To a solution of amide **16** (380 mg, 0.58 mmol) in 20 mL of EtOAc was added MeOH (1.17 mL, 28.9 mmol) followed by dropwise addition of AcCl (2.06 mL, 28.9 mmol) (to generate HCl) at 0 °C. The solution was stirred for 1.5 h at 25 °C, and during that time a precipitate formed. The reaction mixture was filtered to separate the solid product of azidoimidazole hydrochloride salt (240 mg, 99%), which was of sufficient purity for the next reaction: IR (thin film) 3115, 233, 2150, 1611, 1555, 1439 cm^{-1}; ^{1}H NMR (500 MHz, CD_3OD) δ 4.11 (d, J = 5 Hz, 2H), 6.35 (dt, J = 16, 3.5 Hz, 1H), 6.43 (d, J = 16 Hz, 1H), 6.89 (d, J = 2 Hz, 1H), 7.31 (s, 1H); ^{13}C NMR (125 MHz, CD_3OD) δ 42.3 (d, J_{C-N} = 114 Hz), 100.8, 107.3, 115.2, 116.3, 117.5 (d, J_{C-N} = 22.5 Hz), 129.4 (d, J_{C-N} = 106 Hz), 131.8, 132.3, 142.6, 162.4 (d, J_{C-N} = 174 Hz); HRESIMS *m/z* 416.9171 $[M + H]^+$ (calcd for $C_{11}H_{12}Br_2N_6{}^{15}NO$, 416.9163).

To a solution of the azidoimidazole hydrochloride salt (210 mg, 0.50 mmol) in 30 mL of MeOH/EtOAc (1:1) was added Lindlar's catalyst (100 mg, 5% Pd on $CaCO_3$, poisoned with Pb). The resulting mixture was stirred under atmospheric hydrogen at 25 °C for 6 h and then filtered with MeOH through a pad of Celite. The filtrate was concentrated under reduced pressure to leave a residue, which was purified by flash column chromatography on silica gel (gradient elution: 10:1:0 → 1:1:0.01 CH_2Cl_2/MeOH/NH_4OH) to furnish 7-^{15}N-oroidin (**1d**) (165 mg, 84%): IR (thin film) 3304, 2363, 2339, 1620, 1507, 1415 cm^{-1}; ^{1}H NMR (500 MHz, CD_3OD) δ 4.00 (d, J = 6 Hz, 2H), 5.87 (dt, $^{3}J_{NH}$ = 16 Hz, $^{3}J_{HH}$ = 6 Hz, 1H), 6.30 (d, J = 16 Hz, 1 H), 6.47 (s, 1H), 6.83 (d, J = 1 Hz, 1H); ^{13}C NMR (125 MHz, CD_3OD) δ 43.1 (d, $^{1}J_{C-N}$ = 106 Hz), 100.7, 107.0, 115.1, 118.5, 122.2, 123.6 (d, $^{2}J_{C-N}$ = 15 Hz), 129.7 (d, $^{1}J_{C-N}$ = 99 Hz), 132.2, 152.8, 162.4 (d, $^{1}J_{C-N}$ = 175 Hz); HRESIMS *m/z* 390.9289 $[M + H]^+$ (calcd for $C_{11}H_{12}Br_2N_4{}^{15}NO$, 390.9258).

See Supporting Information for additional procedures.

Isolation of Natural Oroidin (1a) from *Stylissa caribica*. A sample of *Stylissa caribica* (wet wt. 24.5 g) was collected in the Bahamas (June 2008) and extracted with 1:1 CH_2Cl_2/MeOH (rt, overnight, 2 × 500 mL). The solvent was removed under reduced pressure and the residue partitioned between hexanes (3 × 250 mL) and 9:1 MeOH/H_2O (250 mL). The aqueous MeOH layer was concentrated and further partitioned between *n*-BuOH (3 × 250 mL) and H_2O (250 mL). Removal of the solvent from the upper layer gave an *n*-BuOH extract (787 mg), a portion of which (191 mg) was adsorbed onto a solid-phase extraction cartridge (C_{18}) and eluted with 4:1 CH_3CN/H_2O, followed by THF. The first-eluting fraction (116 mg) was separated by gradient HPLC (C_{18}, 10:90 to 60:40 CH_3CN/H_2O + 0.1% TFA) to give oroidin **1a** (8.8 mg, 1.0 wt % weight).

MALDI FTMS of Oroidin (1a) and 7-^{15}N-Oroidin (1d). Matrix solution (1 μL of saturated α-cyano-4-hydroxycinnamic acid (CHCA) solution in 50:50:0.2 MeOH/H_2O/TFA) was added to 1 μL of the sample solution (1 pmol/μL) and the sample (approximately 1 pmol) deposited onto a stainless steel target. For each sample, 200 shots were acquired for each mass spectrum (acquisition time, ~1 min each), and 24 spectra were co-added. Data were processed using Bruker software, and error analysis was carried out using standard deviation of replicate MS measurements ($N \geq 5$).

1D ^{1}H−^{15}N HSQC Experiments. Samples for mixing experiments were prepared by addition of measured aliquots of a standard solution of **1d** (1.25 mg/10 mL MeOH) to a sample of **1a** (1500 μg). The samples were concentrated by removal of solvent (MeOH + 0.05% TFA) and redissolved in 1:1 DMSO-d_6/benzene-d_6 (35 μL) before transferring ~30 μL to a NMR tube (ϕ = 1.7 mm) using a gastight syringe. 1D ^{1}H−^{15}N HSQC NMR spectra were acquired with 8K data points in T2 (no zero-fill) and optimized for $^{1}J_{N-H}$ = 90 Hz. Each experiment was preceded by 16 dummy scans, and ~6K scans were collected. The corresponding ^{1}H−^{15}N integrals were averaged and normalized against the N1 pyrrole couplet of **1** (I_P = 1.000). See Table

1 (numbering system follows that of Assman and Köck[32]). $^{1}H-^{15}N$ assignments: δ_H, δ_N (1:1 DMSO-d_6/C_6D_6): 13.14, 169.1 (N1); 8.75, 107.8 (N7); 13.54, 134.7 (N12); 12.78, 137.7 (N14); 8.21, 62.2 (N16).

Acknowledgment. We thank A. Jansma (UCSD) for assistance with NMR, J. Pawlik (UNC Wilmington), and the captain and crew of the RV *Seward Johnson* for logistical support during collecting expeditions and in-field assays. This Investigation was supported by a Ruth L. Kirschstein National Research Service Award NIH/NCI T32 CA009523. We are grateful to the NIH (GM052964 D.R. and T.F.M.) and the Welch Foundation (A-1280) for generous support.

Note Added after ASAP Publication: This paper was published on the Web on Jan 22, 2010, with an omission in the Acknowledgment paragraph. The corrected version was reposted on Mar 1, 2010.

Supporting Information Available: Synthetic procedures and ^{1}H and ^{13}C NMR spectra for **1d**, **9**−**16**, and other intermediates and calculation of LOD for $^{1}H-^{15}N$ HSQC experiments. This material is available free of charge via the Internet at http://pubs.acs.org.

References and Notes

(1) Recent examples of syntheses of pyrrole−imidazole alkaloids: (a) Arndt, H.-D.; Koert, U. In *Organic Synthesis Highlights 4*; Schmalz, H.-G., Ed.; Wiley-VCH: Weinheim, 2000; p 241. (b) Hoffmann, H.; Lindel, T. *Synthesis* **2003**, 1753–1783. (c) Jacquot, D. E. N.; Lindel, T. *Curr. Org. Chem.* **2005**, *9*, 1551–1565. (d) Du, H.; He, Y.; Sivappa, R.; Lovely, C. J. *Synlett* **2006**, 965–992. (e) Kock, M.; Grube, A.; Seiple, I. B.; Baran, P. S. *Angew. Chem.* **2007**, *119*, 6706–6714. (f) *Angew. Chem., Int. Ed.* **2007**, *46*, 6586−6594. (g) Weinreb, S. M. *Nat. Prod. Rep.* **2007**, *24*, 931–948. For some publications not covered in these reviews, see: (h) Dransfield, P. J.; Dilley, A. S.; Wang, S.; Romo, D. *Tetrahedron* **2006**, *62*, 5223–5247. (i) Wang, S.; Dilley, A. S.; Poullennec, K. G.; Romo, D. *Tetrahedron* **2006**, *62*, 7155–7161. (j) Nakadai, M.; Harran, P. G. *Tetrahedron Lett.* **2006**, *47*, 3933–3935. (k) Tan, X.; Chen, C. *Angew. Chem., Int. Ed.* **2006**, *45*, 4345–4348. (l) Overman, L. E.; Paulini, R.; White, N. S. *J. Am. Chem. Soc.* **2007**, *129*, 12896–2900. (m) O'Malley, D.; Yamaguchi, J.; Young, I. S.; Seiple, I. B.; Baran, P. S. *Angew. Chem., Int. Ed.* **2008**, *47*, 3581–3583. (n) Yamaguchi, J.; Seiple, I. B.; Young, I. S.; O'Malley, D. P.; Maue, M.; Baran, P. S. *Angew. Chem., Int. Ed.* **2008**, *47*, 3578–3580. (o) Bhandari, M. R.; Sivappa, R.; Lovely, C. J. *Org. Lett.* **2009**, *11*, 1535–1538. (p) Seiple, I. B.; Su, S.; Young, I. S.; Lewis, C. A.; Yamaguchi, J.; Baran, P. S. *Angew. Chem. Intl. Ed.* **2009**, early view, DOI: 10.1002/anie.200907112.

(2) Al Mourabit, A.; Potier, P. *Eur. J. Org. Chem.* **2001**, 237–243.

(3) Walker, R. P.; Faulkner, D. J.; VanEngen, D.; Clardy, J. *J. Am. Chem. Soc.* **1981**, *103*, 6772–6773. A variation on the sceptrin skeleton, embodying an unusual benzocyclobutane (benzosceptrins A and B), has just been reported: Appenzeller, J.; Tilvi, S.; Martin, M.-T.; Gallard, J.-F.; El-bitar, H.; Dau, E. T. H.; Debitus, C.; Laurent, D.; Moriou, C.; Al-Mourabit, A. *Org. Lett.* **2009**, *11*, 4874–4877.

(4) (a) Keifer, P. A.; Koker, M. E. S.; Schwartz, R. E.; Hughes, R. G., Jr.; Rittschof, D.; Rinehart, K. L. 26th *Interscience Conference on Antimicrobial Agents and Chemotherapy*; New Orleans, Sept 28−Oct 1, 1986; No. 1281. (b) Rinehart, K. L. *Pure Appl. Chem.* **1989**, *6*, 525–528. (c) Kobayashi, J.; Tsuda, M.; Murayama, T.; Nakamura, H.; Ohizumi, Y.; Ishibashi, M.; Iwamura, M.; Ohta, T.; Nozoe, S. *Tetrahedron* **1990**, *46*, 5579–5586. (d) Keifer, P. A.; Schwartz, R. E.; Koker, M. E. S.; Hughes, R. G.; Rittschof, D.; Rinehart, K. L. *J. Org. Chem.* **1991**, *56*, 2965–2975. (e) Williams, D. H.; Faulkner, D. J. *Tetrahedron* **1996**, *52*, 5381–5390.

(5) Nishimura, S.; Matsunaga, S.; Shibazaki, M.; Suzuki, K.; Furihata, K.; van Soest, R. W. M.; Fusetani, N. *Org. Lett.* **2003**, *5*, 2255–2257.

(6) (a) Kinnel, R. B.; Gehrken, H.-P.; Scheuer, P. J. *J. Am. Chem. Soc.* **1993**, *115*, 3376–3377. (b) Kinnel, R. B.; Gehrken, H.-P.; Swali, R.; Skoropowski, G.; Scheuer, P. J. *J. Org. Chem.* **1998**, *63*, 3281–3286.

(7) (a) Bascombe, K. C.; Peter, S. R.; Tinto, W. F.; Bissada, S. M.; McLean, S.; Reynolds, W. F. *Heterocycles* **1998**, *48*, 1461–1464. (b) Urban, S.; de A.Leone, P.; Carroll, A. R.; Fechner, G. A.; Smith, J.; Hooper, J. N. A.; Quinn, R. J. *J. Org. Chem.* **1999**, *64*, 731–735.

(8) Grube, A.; Kock, M. *Org. Lett.* **2006**, *8*, 4675–4678.

(9) D'Ambrosio, M.; Guerriero, A.; Debitus, C.; Ribes, O.; Pusset, J.; Leroy, S.; Pietra, F. *J. Chem. Soc., Chem. Commun.* **1993**, 1305–1306.

(10) D'Ambrosio, M.; Guerriero, A.; Chiasera, G.; Pietra, F. *Helv. Chim. Acta* **1994**, *77*, 1895–1902.

(11) Hong, T. W.; Jímenez, D. R.; Molinski, T. F. *J. Nat. Prod.* **1998**, *61*, 158–161.

(12) (a) De Nanteuil, G.; Ahond, A.; Guilhem, J.; Poupat, C.; Tran Huu Dau, E.; Potier, P.; Pusset, M.; Pusset, J.; Laboute, P. *Tetrahedron* **1985**, *41*, 6019–6033. (b) Poullennec, K. G.; Romo, D. *J. Am. Chem. Soc.* **2003**, *125*, 6344–6345. (c) Imaoka, T.; Iwammoto, O.; Noguchi, K.; Nagasawa, K. *Angew. Chem., Int. Ed.* **2009**, *48*, 3799–3801.

(13) Mason, C. K.; McFarlane, S.; Johnston, P. G.; Crowe, P.; Erwin, P. J.; Domostoj, M. M.; Campbell, F. C.; Manaviazar, S.; Hale, K. J.; El-Tanani, M. *Mol. Cancer Ther.* **2008**, *7*, 548–558.

(14) Foley, L. H.; Büchi, G. *J. Am. Chem. Soc.* **1982**, *104*, 1776–1777.

(15) Baran, P. S.; O'Malley, D. P.; Zografos, A. L. *Angew. Chem., Int. Ed.* **2004**, *43*, 2674–2677.

(16) Baran was unable to convert **2** to **3** under photochemical conditions; however, thermal isomerization of **2** to **3** was achieved under microwave irradiation (195 °C, 1 min, 40% yield and 52% recovered starting material). See ref 15.

(17) Hoffmann, H.; Lindel, T. *Synthesis* **2003**, 1753–1783, and references therein.

(18) (a) Birman, V. B.; Jiang, X.-T. *Org. Lett.* **2004**, *6*, 2369–2371. (b) Papeo, G.; Frau, M. A. G.-Z.; Borghi, D.; Varasi, M. *Tetrahedron Lett.* **2005**, *46*, 8635–8638. (c) Yang, C.-G.; Wang, J.; Jiang, B. *Tetrahedron Lett.* **2002**, *43*, 1063–1066.

(19) (a) Baran, P. S.; Zografos, A. L.; O'Malley, D. P. *J. Am. Chem. Soc.* **2004**, *126*, 3726–3727. (b) Huigens, R. W.; Richards, J. J.; Parise, G.; Ballard, T. E.; Zeng, W.; Deora, R.; Melander, C. *J. Am. Chem. Soc.* **2007**, *129*, 6966–6967.

(20) (a) Nanteuil, G. D.; Ahond, A.; Poupat, C.; Thoison, O.; Potier, P. *Bull. Soc. Chim. Fr.* **1986**, 813–816. (b) Commerçon, A.; Paris, J. M. *Tetrahedron Lett.* **1991**, *32*, 4905–4906. (c) Danios-Zeghal, S.; Mourabit, A. A.; Ahond, A.; Poupat, C.; Potier, P. *Tetrahedron* **1997**, *53*, 7605–7614. (d) Lindel, T.; Hochgürter, M. *J. Org. Chem.* **2000**, *65*, 2806–2809. (e) Berree, F.; Bleis, P. G.; Carboni, B. *Tetrahedron Lett.* **2002**, *43*, 4935–4938.

(21) Lovely, C. J.; Du, H.; Sivappa, R.; Bhandari, M. R.; He, Y.; Dias, H. V. R. *J. Org. Chem.* **2007**, *72*, 3741–3749.

(22) (a) Pirrung, M. C.; Pei, T. *J. Org. Chem.* **2000**, *65*, 2229–2230. (b) Dolensky, B.; Kirk, K. *J. Org. Chem.* **2002**, *67*, 3468–3473.

(23) See the Supporting Information for details.

(24) Deuterium ^{2}H (∼0.02%) and ^{17}O (∼0.04%) also contribute to M + 1, but are much lower in natural abundance (∼0.02% and 0.04%, respectively) and may be ignored in the first approximation.

(25) The $^{13}C/^{15}N$ isotope ratio of *synthetic* and *natural* oroidin samples may differ slightly due to differences in fractionation of ^{13}C (or ^{15}N) in compounds derived by "modern" biosynthesis compared to chemical precursors derived from petrochemical-based feedstock. In practice, this will be inconsequential, since corrections can be made with the appropriate normalization.

(26) The value here, given in commonly used units of $g/2\pi$, was converted from the value cited in the IUPAC 2001 recommendations [$-2.71261804 = g/10^7$ ($rads^{-1}$ T^{-1})]. Harris, R. K.; Becker, E. D.; Cabral de Menezes, S. M.; Goodfellow, R.; Granger, P. *Pure Appl. Chem.* **2001**, *73*, 1795–1818.

(27) Andrade, P.; Willoughby, R.; Pomponi, S.; Kerr, R. G. *Tetrahedron Lett.* **1999**, *40*, 4775–4778.

(28) *Teichaxinella morchella* has synonymity with *Axinella corrugata* and is probably the same as *Stylissa caribica*: http://www.spongeguide.org/speciesinfo.php?species=110.

(29) Stevensine was named in honor of the late Professor Robert V. Stevens (Department of Chemistry and Biochemistry, University of California, Los Angeles). Albizati, K.; Faulkner, D. J. *J. Org. Chem.* **1985**, *50*, 4163–4164.

(30) Englander, J.; Cohen, L.; Arshava, B.; Estephan, R.; Becker, J. M.; Naider, F. *Biopolymers* **2006**, *84*, 508–518.

(31) Assman, M.; Köck, M. *Z. Naturforsch.* **2002**, *57c*, 157–160.

(32) Assman, M.; Zea, S.; Köck, M. *J. Nat. Prod.* **2001**, *64*, 1593–1595.

NP900638E